Distribution of natural radioactivity on the environmental submicronic aerosols

By VRATISLAV HAVLOVIC[1] and JAN OLOF SNIHS[2]

(Manuscript received July 7, 1970; revised version February 11, 1971)

ABSTRACT

An electrial ion mobility analyzer has been built for the study of the environmental aerosol particle size spectrum and of the distribution of natural activity on this spectrum in the size range 10^{-5} cm $> r > 10^{-6}$ cm. The mobility analyzer was carefully tested by a new method to prove the laminarity of flow and the air velocity distribution inside the apparatus. The quantity of charged aerosol particles classified into discrete mobility (or size) groups was estimated by the α-radioactivity of collected particles tagged before entering the analyzer by ThB ions. The electrical mobility analyzer was then completed by a sonic jet diffusion charger for unipolar aerosol charging by diffusion and the elctrical parameters of this device were tested to ensure reliable operation.

The activity size spectra $A(r)$ were transformed to relative particle size distribution curves $N(r)$. The measurements were carried out in Stockholm, Sweden, under varying physical conditions (varying the activity, the residence time, the collector voltage or applying the diffusion charger for unipolar charging of particles). All experiments gave very similar results. The activity curves $A(r)$ of positive and negative particles as a function of radius show a similar profile with a maximum in the region of radius $r = 3$–6×10^{-6} cm corresponding to Junge's model of aerosol particle distribution. The calculated relative particle size distribution curves $N(r)$ are not always characterized by a peak as expected from Junge's model but are increasing below radii $r < 10^{-6}$ cm, so that no peak is evident.

1. Introduction

The environmental inactive aerosol size distribution has been studied by a number of investigators for instance Junge (1953 and 1955), Holl & Mühleisen (1955), Mohnen & Stierstadt (1963) and others using quite different methods. The charge distribution of aerosol particles has been studied by Gunn (1955), Gillespie & Langstroth (1952), Keefe, Nolan and Rich (1959) and others. The attachment coefficient between aerosol particles and small ions has been studied theoretically and/or experimentally by Lassen and Raul (1960), Lassen (1961), Jacobi (1961), Siksna (1963), Fuchs (1963), Baust (1967) and others.

The size range of environmental aerosol particles covers several orders of magnitude in radius with approximate limits of 10^{-3} to 10^{-7} cm. Previously only parts of this spectrum had been investigated due to the size limits of the various experimental methods used. Particle spectra down to radii below 10^{-4} cm are well known as they have been studied by direct count under the optical microscope. Particles of radius less than 10^{-5} cm are counted in total by condensation nuclei counters. However, to deduce nuclei spectra from ion spectra the fraction of charged particles must be known, which just in the region about 10^{-6} cm is not well determined and contains inaccuracies and errors.

At present two methods are useful for the determination of size distribution of natural aerosols in the submicronic region ($r < 10^{-4}$ cm): separation of particles by an electrical field or by centrifugal forces. The method of electrostatic separation with unipolar charging of

[1] Associate Professor, Visiting scientist at the National Institute of Radiation Protection, Fack, S–104 01 Stockholm 60, Sweden.
[2] Senior Physicist, National Institute of Radiation Protection, Fack, S–104 01 Stockholm 60. Sweden.

aerosol particles in a corona discharge has been used by Wilkening (1952), Stierstadt & Papp (1960) and by Salbreiter & Stierstadt (1966). As the electrical charge distribution of particles having passed the corona is disturbed (out of equilibrium), it is quite difficult to use this method for quantitative measurements. Other investigators have used the tagging of aerosol particles by radioactive tracers. This method used originally by Shapiro (1956) and by Chamberlain & Dyson (1956) was improved and used successfully in the estimation of size distribution of the environmental aerosol by Mohnen & Stierstadt (1963). Another type of aerosol particle unipolar charging before the electrostatic separation process has been used by Whitby & Clark (1966) in their "sonic jet diffusion charger".

Another method for the estimation of aerosol particle size distribution is the separation by centrifugal forces. There are two main types of centrifuges for this reason: the Goetz-Aerosol-Spectrometer (Goetz & Kallai, 1962; Goetz & Preining, 1961) and the Conifuge (Sawyer & Walton, 1950; Keith & Derrick, 1960). In spite of some criticism concerning the theory of the Goetz-Spectrometer it has been used by several investigators for the determination of environmental aerosol size distribution in the region $2\ \mu m > r > 0.02\ \mu m$: Schumann (1963), Baust (1967) and Reiter & Carnuth (1967). The Conifuge is not produced commercially and further it is still being developed in order to cover also small particle sizes and to increase its collection efficiency. The results in Conifuge construction announced by Stöber (1967) seem to be quite promising.

Some other methods for the determination of environmental aerosol size distribution are still used, the electron-microscope counting and sizing of particles (Junge, 1953) and the diffusion method (Twomey & Severynse, 1963). Other methods used for the sizing of aerosol particles are the impactor method (Kawano & Nakatani, 1961) and filter pack method (Schleien Friend & Thomas, 1967). These do not deliver exact results as they are sizing the aerosol particles in a limited range into a few groups only.

In our investigations of the environmental aerosol particle size distribution, carried out in Stockholm, we were interested in the region $10^{-5}\ cm > r > 10^{-6}\ cm$, and we have chosen the method of electrical separation of aerosol particles previously tagged by the decay products of thoron.

2. Experimental arrangement

2.1 *Electrical mobility analyzer*

The present experience from published results showed that for aerosol particle sizing in the region $10^{-5}\ cm > r > 10^{-6}\ cm$ the electrostatic method has many advantages. The ion mobility of charged aerosol particles is usually measured by passing the aerosol in a laminar stream through a cylindrical condenser in which a radial electrical field perpendicular to the direction of aerosol flow is maintained. This radial electrical field precipitates the charged particles on the condenser electrodes permitting the particle mobility to be calculated.

The samples thus obtained are primarily classified according to the ion mobility of the aerosol particles. To get a spectrum according to the particle size, it is necessary to assume that the particle mobility is a single valued function of its particle size (valid for particle radius $r < 2 \times 10^{-6}$ cm), or a correction for multiply-charged particle fraction is necessary or the aerosol particles must be charged artificially so that the condition of single charged particles is fulfilled (Whitby & Clark, 1966). The relation between ion mobility and particle radius can be calculated from equations or estimated from figures published by Israël (1957).

2.1.1 *Theory of an electrical mobility analyzer of cylindrical type.* For the measurement of the ion mobility spectrum the air flow in the mobility analyzer must be exactly laminar and the velocity over the cross-section might have a particular profile unchanged along the axis of the chamber. The flow of a viscous incompressible medium between two concentric tubes is described by the Navier-Stokes' equation:

$$\eta \cdot l \cdot \frac{dv(r)}{dr} + \eta \cdot l \cdot r \cdot \frac{d^2v(r)}{dr^2} = -r\Delta p \qquad (1)$$

where η = dynamic viscosity, l = length of the tube, $v(r)$ = velocity at radius r, Δp = pressure difference between the opposite ends of the tube. The equation (1) is valid for laminar flow and for a tube of a certain length, where the beginning disturbances at the orifice are smoothed.

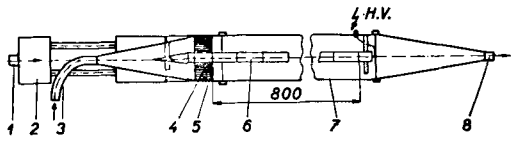

Fig. 1. Electrical aerosol mobility analyzer. *1*, aerosol input; *2*, dividing chamber; *3*, clean air input; *4*, flow straightening rings; *5*, circular slit; *6*, central collector rod (electrode); *7*, outside cylinder (electrode); *8*, aerosol output; *H. V.*, high voltage.

The velocity distribution which is built up does not change as a function of the length of the tube.

The Navier-Stokes equation (1) can be used for the calculation of the air velocity distribution (Petrausch, 1967). After integration of equation (1) another equation for velocity distribution is obtained:

$$v(r) = -\frac{\Delta p}{4\eta l} r^2 + C_1 \ln r + C_2 \qquad (2)$$

where the constants C_1 and C_2 are estimated by the initial conditions (where r_1, r_2 = radius of the outer and inner cylinder):

$$v(r_1) = 0 \qquad v(r_2) = 0 \qquad (3)$$

If the arbitrary distribution of stream-velocity is supposed to be $v(r)$, the flow-rate Q is expressed as follows

$$Q = 2\pi \int_{r_2}^{r_1} v(r)\, r\, dr = 2\pi [F(r_1) - F(r_2)] \qquad (4)$$

where $F(r) = \int v(r)\, r\, dr$. The trajectory of an ion can be written as

$$\frac{dx}{dr} = \frac{dx}{dt} \cdot \frac{dt}{dr} = v(r) \left(-\frac{1}{kE} \right)$$

$$\frac{dx}{dr} = -\frac{\ln r_1/r_2}{kU} \cdot v(r) \cdot r \qquad (5)$$

where k = mobility of an ion, E = electrical field, U = potential difference between the outer and inner cylinder and x = distance from the entrance along the axis. Integrating equation (5) we obtain

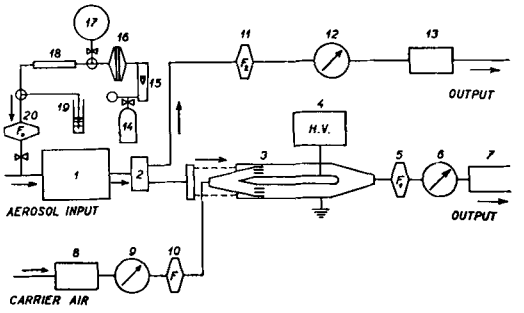

Fig. 2. Schematic of the electric aerosol mobility analyzer with auxiliary equipment. *1*, large mixing chamber (volume 480 l); *2*, small mixing chamber (volume 28 l); *3*, mobility analyzer; *4*, high voltage source; *5*, F_1 filter; *6*, gasmeter; *7*, air-blower; *8*, air-blower; *9*, gasmeter; *10*, absolute filter; *11*, F_2 filter; *12*, gasmeter; *13*, air-blower; *14*, compressed air cylinder; *15*, flow-meter; *16*, dry thoron-source; *17*, rubber-balloon; *18*, decay-tubes; *19*, bubble-chamber; *20*, F_0 filter.

$$x = -\frac{\ln r_1/r_2}{kU} \int v(r)\, r\, dr$$

$$x = -\frac{\ln r_1/r_2}{kU} [F(r) + F^1] \qquad (6)$$

For initial conditions $r = r_1$ at $x = 0$ (aerosol inlet) then follows

$$F^1 = -F(r_1)$$

Critical mobility k_c is obtained by putting $r = r_2$ and $x = l$ (where l = length of the central electrode)

$$k_c = \frac{\ln r_1/r_2}{lU} [F(r_1) - F(r_2)] \qquad (7)$$

$$k_c = \frac{\ln r_1/r_2}{lU} \cdot \frac{Q}{2\pi} \qquad (8)$$

This shows that the critical mobility k_c does not depend on the velocity distribution but on air flow-rate. The critical mobility is characterized by the dimension ($cm^2 \times sec^{-1} \times volt^{-1}$); it means that with a given potential difference U between the electrodes all charged particles or ions with a mobility $k \geq k_c$ are attached to the central electrode.

2.1.2 *Construction of an electrical mobility analyzer.* We used an electrical mobility analyzer of cylindrical type, Fig. 1, which was in princi-

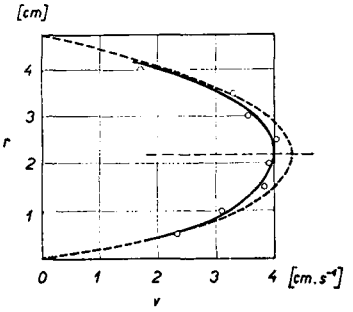

Fig. 3. The air velocity distribution inside the mobility analyzer. Experimental curve (——), calculated curve (– – – –).

ple similar to that described by Mohnen & Stierstadt (1963). The charged aerosol particles (pos. or neg. sign) were precipitated on the central collector rod with 10 rings. To get the collected particles on this rod easily for radiation measurement, 10 pieces of thin (0.1 mm) aluminium foil were attached to the rings of the central collector rod and after removal from the rod they were counted for α-radioactivity.

The whole arrangement is shown in a schematic form in Fig. 2. Before entering the mixing chamber (*1*) with a volume 480 l the environmental aerosols were tagged by ThB-radioactivity from a dry thoron source (*16*). Some decay tubes (*18*) were used for decreasing the activity of thoron and before entering the pipe into the mixing tank all decay-products of thoron were removed in filter F_0 (*20*). In the mixing chamber (*1*) the decay products of thoron became attached to the aerosol particles and afterwards the aerosol stream was led into the second chamber (*2*) with volume 28 l where the flow was divided into two parts. One part continued through filter F_2 (*11*) and enabled an estimate to be made of the activity in the large mixing tank (*1*). The other part continued to the electrical mobility analyzer (*3*).

As filter-material we have used for filters F_1 and F_2 the Gelman GA3 membrane 1.2 μ filter with a diameter $\varnothing$ 100 mm. The same type of filter but with smaller diameter $\varnothing$ 26 mm has been used for F_0 in the thoron line. For carrier air line an absolute glass-fiber filter of type Gelman Glass Fiber "A" of $\varnothing$ 100 mm diameter has been used.

The flow rates used in all experiments were adjusted to these values: the aerosol input to the mobility analyzer $Q_a = 2.88$ l/min, the carrier-air input $Q_0 = 18$ l/min and the analyzer output $Q_t = 20.88$ l/min. At these flow-rate values the original equation (8) reduces to a simple relation for the center of each ring of the central rod (impaction point):

$$k_c = a_i \frac{1}{U} (\mathrm{cm^2\,sec^{-1}\,volt^{-1}}) \qquad (9)$$

where U = voltage on the inner electrode (the outer electrode was earthed), a_i = constant summarized for the 10 impaction points ($i = 1$–10) as follows:

i	1	2	3	4	5
a_i	20.00	6.67	4.00	2.81	2.22
i	6	7	8	9	10
a_i	1.82	1.56	1.33	1.18	1.05

The collecting orifice of the aerosol input was situated about 2 m above the ground outside a low laboratory building.

2.1.3 *Experimental determination of air velocity distribution.* The velocity distribution, calculated from the theory presented above (equations (2) and (3)) for our geometric arrangement and the total flow-rate $Q_t = 20.88$ l/min is illustrated in Fig. 3 (– – – –).

An experimental estimation of air velocity distribution was tried at first by a method developed for this purpose by Misaki (1960). The air flow pattern and velocity distribution inside the mobility analyzer had to be proved with the aid of streams or puffs of smoke introduced into the air stream. For this purpose the outside metal cylinder was replaced by a transparent perspex one which allowed optical inspection of the flow pattern inside the mobility analyzer. For creating smoke puffs a special device was constructed. If the period of chopping is known, the velocity of the air can be determined by measuring the distance of successive puffs with the aid of photography at different positions between the outer and inner cylinder, where the glass nozzles ejecting smoke puffs were fixed. As the photographic method proved troublesome in practice we have chosen a quite simple method of optical inspection and measuring the velocity of the smoke puffs at varying radial distances on a defined length base (parallel to analyzer axis). The linear velocity $v(r)$ as a function of the radial distance r showed

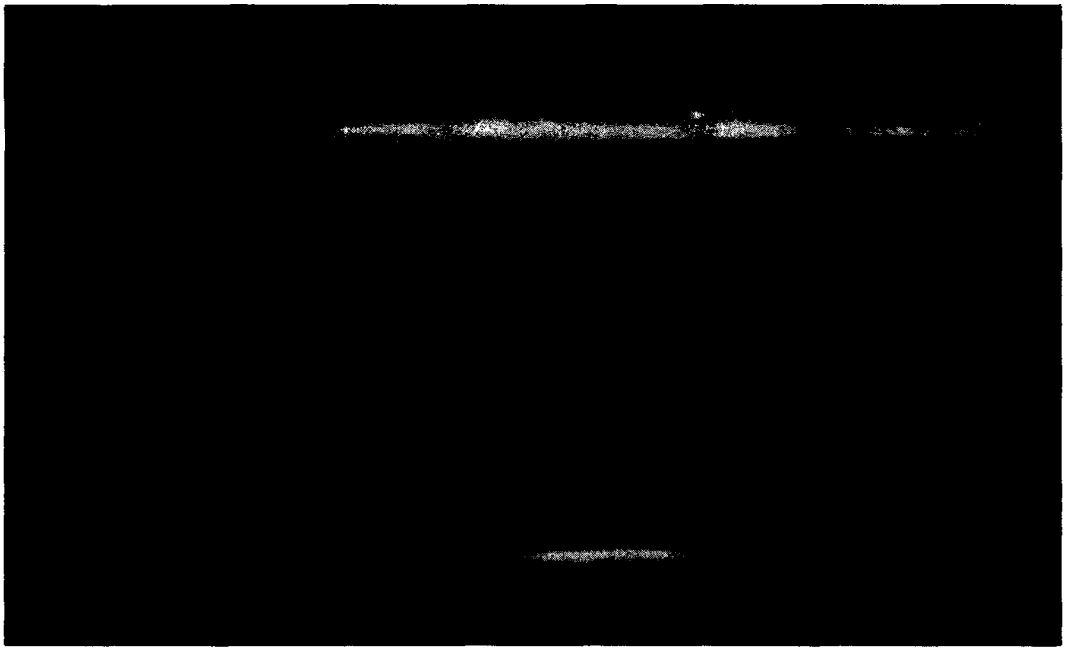

Fig. 4. Smoke plume in a laminar air-flow. The flow-rate is 20.88 l/min.

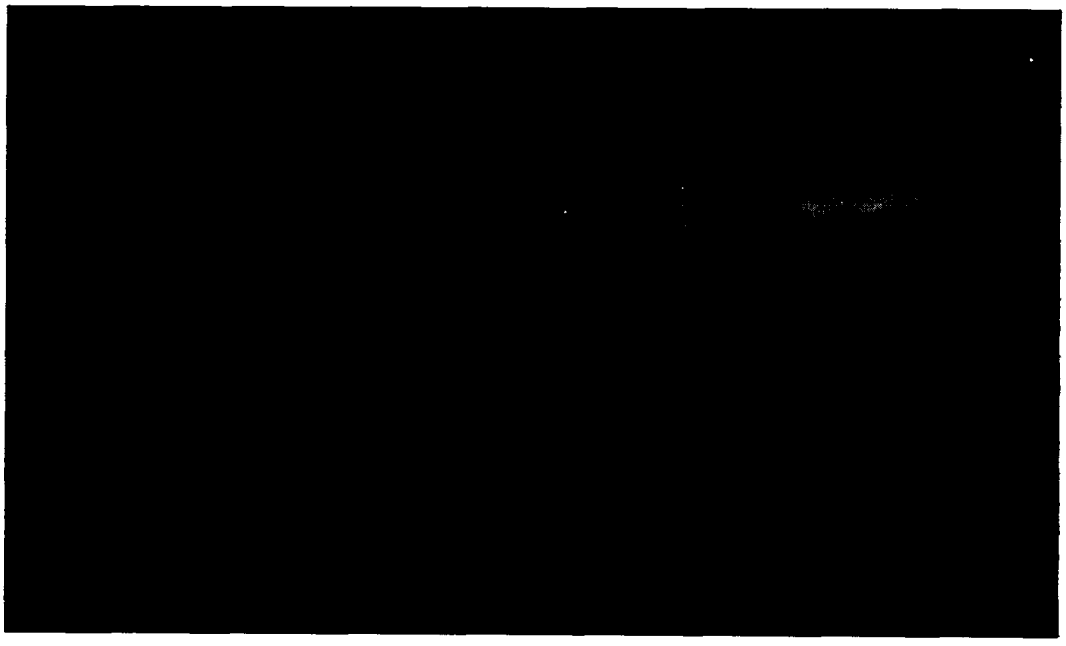

Fig. 5. Smoke plumes in a turbulent air-flow.

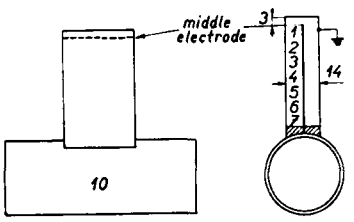

Fig. 6. Collecting device with two electrodes for tracer laminarity experiment.

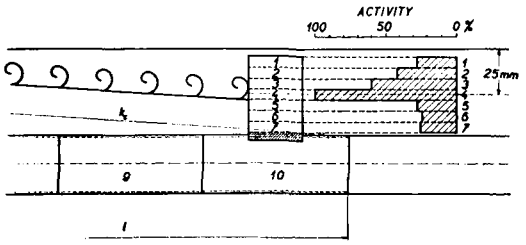

Fig. 7. Activity measurement on the collecting device put into the mobility analyzer instead of the 10th collector ring.

a parabolic relationship as shown in Fig. 3 —— The mean linear velocity $\bar{v}$ calculated from the air flow-rate Q_t is 2.8 cm sec^{-1}. Comparison with the Reynold's formula for critical velocity $\bar{v}_{crit}$, when laminar flow converts to turbulent one, indicated that the mean velocity used $\bar{v} = 2.8$ cm/sec is under the critical velocity $\bar{v}_{crit} = 22$ cm/sec (for an ideal pipe with convenient margin) for the dimensions of this analyzer. The behaviour of smoke plumes inside the mobility analyzer showed clearly the pattern of air-flow at different radial distances from the central rod (white base line on Figs. 4–5). When the air-flow is laminar (Fig. 4) the smoke plumes are stright lines without remarkable increasing of their width. At high air flow-rate (Fig. 5) the smoke streaks disappear under the mixing action of turbulence.

As a complement to the described optical observations a further control experiment was carried out using a radioactive tracer. At the place for the last 10th ring on the central electrode (corresponding to the minimum ion mobility) a collecting device was mounted as shown in Fig. 6. This device consisted of one outer electrode (earthed) and one middle electrode connected to a -200 V battery. The experiment was carried out under the same conditions as in the subsequent aerosol experiments, i.e. with aerosols tagged by ThB atoms. However, no voltage was applied to the analyzer (between the central electrode and the outer cylinder wall). The α-activity was then measured on the central plate of the collecting device in seven strips step by step. The result is illustrated in Fig. 7. The conclusion was that the aerosol stream from the cylindrical slit diffuses towards the central electrode during its passage through the analyzer, not, however, to such an extent that it with any significance reaches the central electrode. The ions with critical mobility $k \geq k_c$ are moving on a parabolic path inside the laminar carrier air. This is of great importance with regard to the experimental conditions essential for the subsequent aerosol experiments.

2.2 *Supplementary apparatus*

2.2.1 *Radioactive dry thoron emanating source.* As a thoron generator for aerosol particle tagging a dry source of radio-thorium (Th^{228}) prepared by the method of Hursh & Lovaas (1967) has been used. The activity of our source of Th^{228} type RLS 1 (delivered by the Radiochemical Centre Amersham, England) was about 0.58 mCi Th^{228}. The recommended air flow through the source is about 10 l/h. The output activity of thoron and its decay products was varying with the number of decay tubes used in the experiment.

In all measurements of the ThB-activity the α-measurement on its decay-products ThC + ThC^1 was used and therefore some corrections

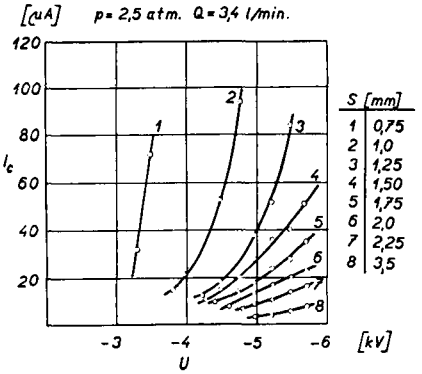

Fig. 8. Sonic jet diffusion charger. Corona current I_c as function of corona voltage U; needle-to-orifice spacing S as parameter. Pressure p and flow-rate Q of compressed air constant.

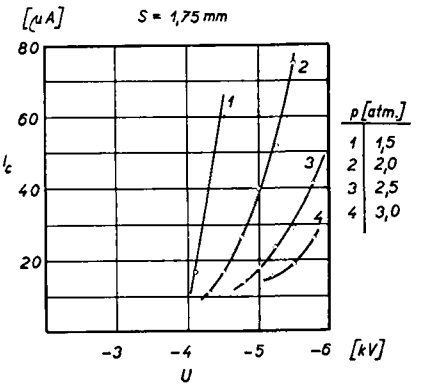

Fig. 9. Sonic jet diffusion charger. Corona current I_c as function of corona voltage U; pressure p of compressed air as parameter. Needle-to-orifice spacing S constant.

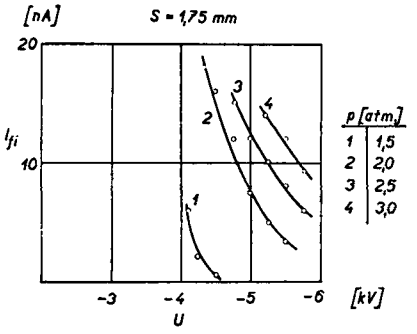

Fig. 10. Sonic jet diffusion charger. Free ion current I_{fi} output as function of corona voltage U; pressure p of compressed air as parameter. Needle-to-orifice spacing S constant.

were necessary (Evans, 1955). Our ThB activity values are valid at time $t = 0$ (at the end of the experiment) and therefore a further correction for the decay of ThB was necessary.

2.2.2 *Sonic jet diffusion charger.* The ion mobility analyzer is capable of separation of charged particles only; for the estimation of the uncharged fraction of atmospheric aerosol in the measured size-range further theoretical calculations are necessary. For a direct measurement of this uncharged fraction the uncharged particles must be charged. Whitby & Clark (1966) used for this purpose unipolar negative charging by a special diffusion charger called "sonic jet diffusion charger". We have used this design of the diffusion charger in some of our experiments. Negative ions generated by a sonic jet corona generator (Whitby, 1961) are ejected downward through a small orifice (0.35 mm) in the metal anode into a conical space where they mix with the aerosols entering from an annular slot. The entering aerosols are charged by diffusion as they mix with the ions. A plastic cone leads the charged aerosol particles to the storage vessel. The total free ion current I_{fi} is monitored by a vacuum tube voltmeter with high input resistance (Hewlett Packard mod. 425A) connected between the charging chamber and the earth.

The operation of the charger was tested by examining its electrical parameters. At first the dependence of corona current I_c on corona voltage U was estimated at various needle to orifice spacings S (Fig. 8). Then free ion current I_{fi} output as a function of corona voltage U at various needle to orifice spacings S was tested. Further the corona current I_c as function of corona voltage U at varying compressed air pressures p was measured (Fig. 9). In Fig. 10 the free ion current I_{fi} as a function of corona voltage U at different pressures p is illustrated. Finally Fig. 11 shows the corona current I_c and free ion current I_{fi} as function of the pressure p at constant needle to orifice spacing S and constant corona voltage U. From the characteristics illustrated in Fig. 8–11 the following values were chosen as operational parameters: corona voltage $U = 5$ kV, needle to orifice spacing $S = 1$ mm, pressure $p = 2.5$ atm at $Q = 3.4$ l/min. Using the sonic jet diffusion charger for unipolar aerosol charging the apparent

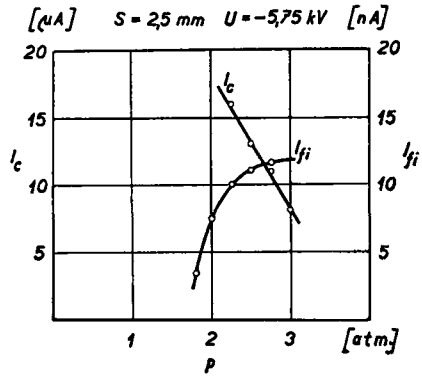

Fig. 11. Sonic jet diffusion charger. Corona current I_c and free ion current I_{fi}, as function of pressure p of compressed air at constant needle-to-orifice spacing S and constant corona voltage U.

particle count then delivered by the mobility analyzer should be corrected by a factor C (single efficiency factor depending on particle radius r), which takes into account the combined space charge loss and charging efficiency as recommended by Whitby & Clark (1966). The useful lower particle size limit of the instrument is about radius $r = 8 \times 10^{-7}$ cm, since the fraction charged and collected rapidly approaches zero below this size.

3. Measurement of environmental aerosols

3.1 *Method of particle size evaluation*

For the evaluation of the activity curves $A(r)$ of positive and negative particles delivered by the electrical mobility analyzer as a function of their ion mobility the process of attachment of radioactive ions and atoms to aerosol particles must be known. The theory of attachment published by Baust (1967) was adapted especially for the attachment of ThB ions and atoms which were used in our experiments for radioactive tagging. The calculated attachment coefficients of ThB ions and of ThB neutral atoms were then applied for a special case of charge distribution, symmetric bipolar aerosol. For all radii the number of positive and negative charges are the same in this case. The total attachment coefficients $\eta(r)$ for ThB were calculated by Baust as a function of aerosol particle radius. With the aid of a known charge distribution (supposed to be symmetric) and of the total attachment coefficients for ThB the total particle size spectrum can be estimated.

At first the activity distribution as a function of impaction point (the distance on the central electrode from the zero point) must be converted with the aid of equation (9) to the activity distribution as a function of ion mobility. Using the known relation between the radius and ion mobility of the charged particles (Israël, 1957) this distribution can be further converted to the activity distribution as a function of radius. All particles are estimated to carry one elementary charge. Further correction to a constant radius interval Δr must be made as the constant length interval Δl does not correspond to a constant radius interval Δr.

The correction to multiple charged particles should be made as the double, triple and multiple charged particles are deposited at different impaction points. This correction for multiple charged particles was not used in our evaluation. The error introduced in the region between 10^{-5} cm $- 5 \times 10^{-6}$ cm is estimated to be about 10–15 %; in the region below 5×10^{-6} cm it is much lower.

Assuming that the symmetric bipolar charged aerosols are not changed by the ThB attachment, dividing the activity spectrum $A(r)$ by the total attachment coefficient $\eta(r)$ we get the fraction $N_p(r)$ of the charged aerosol of radius r. The total number, $N(r)$, of particles of radius r can be deduced from the charged fraction from the equation

$$N(r) = P(r) \sum_{p=1}^{\infty} N_p(r) \tag{10}$$

where

$$P(r) = \frac{N_0(r)}{\sum_{p=1}^{\infty} N_p(r)} + 2 \tag{11}$$

The first term in eq. (11) can be calculated from the known fractions of p-times charged aerosol particles in a symmetric bipolar aerosol. Whenever the activity curves $A(r)$ of both polarities of particles were available the positive curve was used for particle size distribution.

3.2 *Technique of collection*

Our measurements of environmental aerosol size distribution were made at the National Institute of Radiation Protection in Stockholm during summertime and they consisted of 32 experiments. The experiments ran from 16.00 hours overnight till 09.00 hours in the morning, that is 17 hours. At night the aerosol composition is quite stable as Hasenclever & Siegmann (1960) demonstrated, although during the day it varies depending on the meteorological conditions and artificial influences. Our experimental conditions were constant: aerosol flow rate $Q_t = 20.88$ l/min, the voltage between the electrodes $U = \pm 100$ V, ± 1 kV, ± 10 kV. All drifts in the flow-rate or in the voltage between the electrodes were corrected so that they did not influence any mobility shift. The activity of ThB used in the mixing chamber was chosen at three different values: $A_1 = 120 \cdot 10^{-10}$ Ci/m^3 ± 10 %, $A_2 = 20 \cdot 10^{-10}$ Ci/m^3 ± 27 % and $A_3 = 2.6 \cdot 10^{-10}$ Ci/m^3 ± 13 %. Two values were adopted for the residence time of the environ-

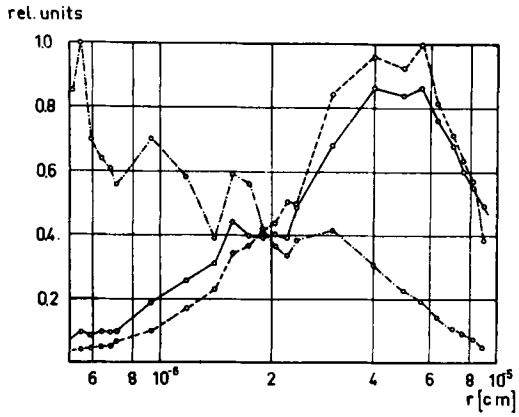

Fig. 12. Activity of positive (——) and negative (- - - -) charged particles as a function of particle radius r. Relative particle size distribution of an environmental aerosol (-·-·-·-). Activity of ThB $A_1 = 120 \times 10^{-10}$ Ci/m³ ± 10 %, residence time T_{R1} = 88.2 min (Series A).

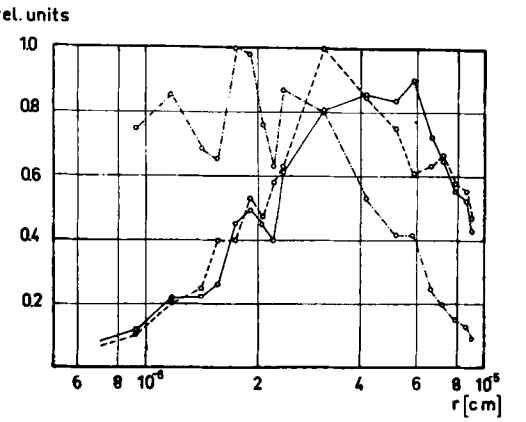

Fig. 13. Activity of positive (——) and negative (- - - -) charged particles as a function of particle radius r. Relative particle size distribution of an environmental aerosol (-·-·-·-). Activity of ThB $A_2 = 20 \times 10^{-10}$ Ci/m³ ± 27 %, residence time T_{R1} = 88.2 min (Series B).

mental aerosols in the large mixing chamber: $T_{R1} = 88.2$ min, $T_{R2} = 10$ min. Also the filters F_1 and F_2 were measured. All the α-measurements were arranged 5 hours after the end of collection. The activitites were expressed as ThB activity at the end of collection ($t = 0$).

Our measurements of environmental aerosols consisted of five series using different experimental conditions (using tagging by ThB):

Series	Activity	Residence time (min)
A	$A_1 = 120 \cdot 10^{-10}$ Ci/m³ ± 10 %	T_{R1}(88.2)
B	$A_2 = 20 \cdot 10^{-10}$ Ci/m³ ± 27 %	T_{R1}(88.2)
C	$A_3 = 2.6 \cdot 10^{-10}$ Ci/m³ ± 13 %	T_{R2}(10)
D	$A_4 = 1.73 \cdot 10^{-10}$ Ci/m³ ± 3.1%	T_{R2}(10)
E	$A_5 = 3.95 \cdot 10^{-10}$ Ci/m³ ± 3.9%	T_{R2}(10)
F	Natural activity	

Series A–C were arranged using different collector voltages (±100 V, ±1 kV, ±10 kV) corresponding to three ion mobility ranges (for both signs):

1) 10^{-1} to 10^{-2} cm² sec^{-1} volt^{-1} (±U)
2) 10^{-2} to 10^{-3} cm² sec^{-1} volt^{-1} (±U)
3) 10^{-3} to 10^{-4} cm² sec^{-1} volt^{-1} (±U)

The three curves of every sign were then put together and a complete mobility curve for positive and negative particles ranging from $10^{-1} - 10^{-4}$ cm² sec^{-1} volt^{-1} was obtained. Series D was a control measurement where another collector voltage was used (+500 V, +5 kV) to prove whether the curve corresponds to that of the previous experiments. Series E was made with the aid of the sonic jet diffusion charger, characterized by unipolar negative charging of particles. Series F was made with particles carrying the natural radioactivity only (without previous tagging by ThB) at mean activity value $A_0 = 0.18 \times 10^{-10}$ Ci/m³ ± 25 %. In this last case the results are—as expected—uncertain because of low activity. The mean S.D. σ in the α-radioactivity measurements is 9 %, if Series F is excluded. Thirteen per cent of the measurement points has a S.D. of more than 15 % but less than 27 % (max.) preferably in the size region $< 10^{-6}$ cm. Series F has a mean S.D. of 32 % (42 % in the region $< 2 \times 10^{-6}$ cm and 18 % in the region $> 2 \times 10^{-6}$ cm).

3.3 *Experimental results*

As a first step the activity of postive (——) and negative (- - - -) charged particles as a function of particle radius r was estimated by the process described in the previous chapter 3.1. The results for different experimental conditions

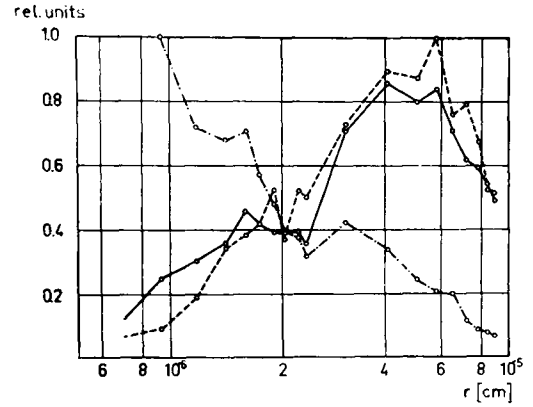

Fig. 14. Activity of positive (——) and negative (·---) charged particles as a function of particle radius r. Relative particle size distribution of an environmental aerosol (–·–·–·–). Activity of ThB $A_3 = 2.6 \times 10^{-10}$ Ci/m³ ± 13 %, residence time $T_{R2} =$ 10 min (Series C).

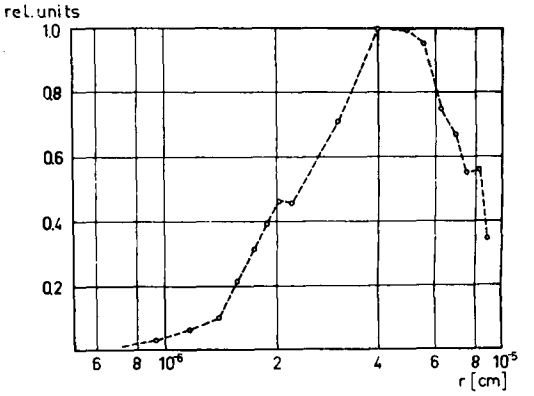

Fig. 16. Activity of negative charged particles as a function of particle radius r. Activity of ThB $A_5 = 3.95 \times 10^{-10}$ Ci/m³ ± 3.9 %, residence time $T_{R2} =$ 10 min (Series E), unipolar charging (Whitby).

(Series A–F) are presented in Figs. 12–17. All of the curves show similar profiles and a maximum dominating the region between radius $r = 3$–6×10^{-6} cm can be observed. One exception is in Series F (natural activity distribution), where the curve increases towards the upper end of the diagram ($r = 10^{-5}$ cm), but as mentioned above the results of Series F are not absolutely reliable because of the low activities. From the similar results presented in Figs. 12–16 (Series A–E) we can draw these conclusions:

1. The results obtained were dependent neither on the ThB activity used for particle tagging nor on the aerosol residence time in the large mixing chamber (Series A–C). Although the ThB activity was varied by a factor of 6, no alteration in the activity distribution curve has been observed; the same applies to the variation of residence time by a factor of 8.8.

2. The operation of the apparatus is reliable at different collector voltages (comparison of Series A–C to Series D).

3. The operation of the mobility analyzer in connection with the sonic jet diffusion charger for unipolar charging of all aerosol particles (Series E) is quite satisfactory.

4. The size distribution of the environmental aerosols especially during the nights when our measurements were arranged seems to be quite stable within the size region of radius $10^{-5} > r > 10^{-6}$ cm.

5. The reproducibility and reliability of the apparatus has been verified by the good agreement found in the comparison of activities of filters F_1 and F_2 to the summed activities $\sum_{A_i}^{\pm U}$ of individual rings ($i = 1$–10) on the central collector electrode at voltage $\pm U$.

In the experiments Series A–C the activity of negative charged particles (ions) especially in the region of the peak ($r = 3$–6×10^{-6} cm) is higher than that of positive charged particles. The ratio of activity of negative to positive

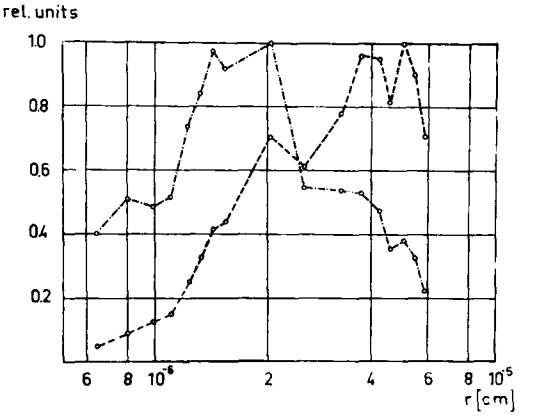

Fig. 15. Activity of negative charged particles as a function of particle radius r. Relative particle size distribution of an environmental aerosol (–·–·–·–). Activity of ThB $A_4 = 1.73 \times 10^{-10}$ Ci/m³ ± 3.1 %, residence time $T_{R2} = 10$ min (Series D).

Size group (radius)		pos. (%)	neg. (%)
Small middle ions	$(2.4 \times 10^{-7}\,\text{cm} < r < 7.8 \times 10^{-7}\,\text{cm})$	5.6	2.7
Large middle ions	$(7.8 \times 10^{-7}\,\text{cm} < r < 2.5 \times 10^{-6}\,\text{cm})$	27.9	23.4
Langevin ions	$(2.5 \times 10^{-6}\,\text{cm} < r < 5.7 \times 10^{-6}\,\text{cm})$	41.3	47.1
Ultra-large ions	$(r > 5.7 \times 10^{-6}\,\text{cm})$	25.2	26.8

particles in the peak region increases with increasing activity inside the mixing chamber. This can be explained as follows. The mobility of negative ions is higher than that of positive ions. With increasing activity inside the mixing chamber there is increased ionization and the maximum of charge distribution is moving to the negative side as a consequence of the unequal mobility of ions.

A further interesting region in the activity-particle size spectrum seems to occur in the region of $r = 2 \times 10^{-6}$ cm, where a small secondary peak appears in the particle-curves (Series A–C). This secondary peak can also be observed in Series D–E. Below this secondary activity peak towards radii $r < 2 \times 10^{-6}$ cm (mobilities $K > 1.7 \times 10^{-3}$ cm^2 sec^{-1} volt^{-1}) the activity curves of negative particles are crossing the activity curve of positive particles so that below $r = 10^{-6}$ cm the activity curve of positive particles dominates that of the negative particles.

By planimetric comparison of different particle size groups according to Israël's classification (1957) of ions we can find the distribution for positive and negative particles in Series A (se above).

In Fig. 18 our results are compared with published data of other investigators using different methods. In this figure the theoretical conclusions are illustrated together with experimental results as integral activity distribution curves of atmospheric aerosols, that is the integrated activities of all particles with radii smaller than r as a function of r. Both full curves in Fig. 18 are calculated applying Lassen's attachment formula (1961) for the influence of electrical forces on the attachment process on two different models of inactive aerosol size distribution: the Junge's model (1962) and Holl–Mühleisen's model (1955). As Schumann (1963) presented, all the experimental results published

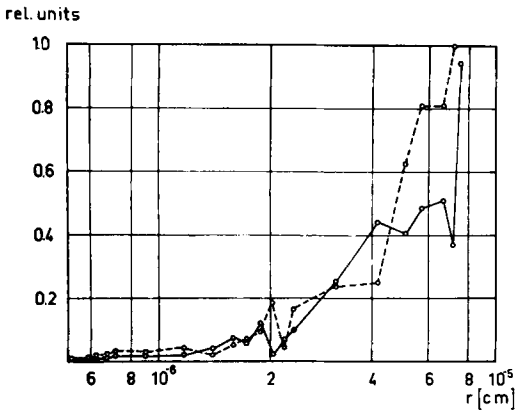

Fig. 17. Natural activity of positive (——) and negative (- - - -) charged particles as a function of particle radius r. Natural activity $A_0 = 0.175 \times 10^{-10}$ Ci/m^3 $\pm$ 24.7 %.

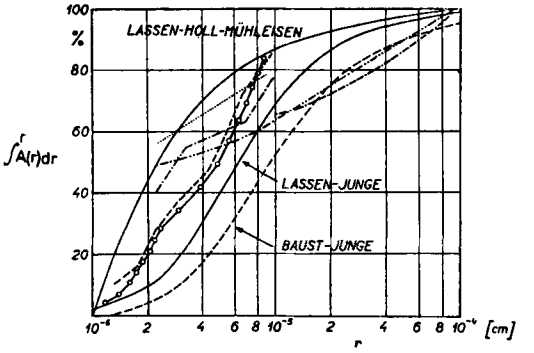

Fig. 18. Integral activity distribution in the atmospheric aerosol. *Upper curve*: Lassen's attachment formula (1961) applied to Holl–Mühleisen's aerosol distribution model (1955); *lower curve*: Lassen's attachment formula applied to Junge's aerosol distribution model (1962); - - - -, Baust's attachment coefficient (1967) applied to Junge's aerosol distribution model; —·—·—·, Schumann (1963) natural radioactive aerosol; —··—··—, Schumann (1963) aerosol tagged by ThB; ...., measurements by Bricard; ——·——·, measurements by Wieser (1966); — — — —, measurements by Mohen & Stierstadt (1963); O–O–O–O, measurements published in this paper (Series A).

by different investigators and transformed to integral activity distribution curves $\int^r A(r)\,dr$ are with few exceptions located between Junge's and Holl–Mühleisen's curve (see Fig. 18). This fact is verified by activity distribution curves published by Schumann (1963) (on natural radioactive aerosols and on aerosols tagged by ThB), also by integral activity curves derived from papers of Bricard (1965), of Wieser (1966) and of Mohnen & Stierstadt (1963). Our own results, calculated from Series A, are most similar to the integral activity distribution curves of Mohnen & Stierstadt in spite of different geographical and climatic conditions; this might be explained by similar methods (electrical mobility analyzer) used in both measurements. The methods used seem to influence the results even in other cases: comparable results were also obtained by Schumann (1963) and of Wieser (1966) with tagging of particles by ThB.

The activity distribution curves were then transformed to relative particle size distribution curves $N(r)$ (dot-dashed curves in Figs. 12–15). The particle size distribution curves do not show the significant peak predicted by the Junge's model of aerosol size distribution. The particle size distribution curve increases for smaller particles (Fig. 12. and 14) or seems to reach a constant value (Fig. 13). This observation is not in agreement with the results of Mohnen & Stierstadt (1963) either. Towards larger particle sizes the rapid decrease of the particle size distribution curve corresponds to Junge's aerosol distribution model. In the particle size distribution curve in Fig. 15 (Series D) a peak in the region $r = 2 \times 10^{-6}$ cm can be detected.

4. Discussion

The environmental aerosol particle size distribution is an object of intensive investigation from different points of view and therefore many papers on this subject have been published in the last few years. The indirect methods for these investigations are quite different in principal from the direct observation of submicronic particles which is only possible by electron microscopy. Furthermore, the results differ from each other and it is difficult to distinguish the differences originating from different methods from those resulting from differing conditions in the environment.

The electrical mobility analyzer used in our studies operates in the region of particle radii 10^{-5} cm $> r > 10^{-6}$ cm. At first we have proved the operational characteristics of this mobility analyzer and especially the laminarity of the air flow. The air velocity distribution calculated from Navier-Stoke's equation was in good agreement with experimental results obtained in smoke tests. A new method using radioactive tracing of aerosol particles with ThB enabled us to determine the laminarity of air flow inside the mobility analyzer. Careful laminarity tests proved the reliable operation of the analyzer. Further a radioactive dry thoron emanating source has been built and the delivered activity measured by different methods; estimation of ThB activity was arranged by the α-measurement of ThC + ThC[1].

For unipolar aerosol charging by diffusion we used a sonic jet diffusion charger and examined operational electrical parameters. As we could not estimate the efficiency factor of this device (especially valuable for small particles with radii $r < 2 \times 10^{-6}$ cm where the collection efficiency decreases rapidly), we used the factor published by Whitby & Clark (1966).

The theoretical calculations by Baust (1967) for the attachment of radioactive ions and atoms to aerosol particles are at present the most advanced theory in this field, which takes all the factors influencing the attachment process into account. We have therefore used the total attachment coefficient of ThB for a symmetric bipolar aerosol from Baust's theory in the evaluation of our experiments. By this method the calculation of the particle size spectrum $N(r)$ from the activity spectrum $A(r)$ does not deliver absolute values of particle concentrations as a function of particle radius.

All our measurements of environmental aerosols delivered very similar results (Series A–E), even with varying physical conditions. The activity curves $A(r)$ of positive and negative particles as a function of radius r in the size range 10^{-5} cm $> r > 10^{-6}$ cm show a similar profile with a maximum in the region of radius $r = 3\text{–}6 \times 10^{-6}$ cm. The night sampling was essential to ensure a constant aerosol size spectrum for our experiments. Changes in the ThB activity by a factor of 6 and variation of residence time by a factor of 8.8 did not influence the results. Operation of the mobility analyzer with different collector voltages and

unipolar diffusion charging did not alter the profile of the activity curves. As proved by our measurements the results of direct estimation of the environmental radioactive aerosol distribution by measuring its natural activity in different size groups are not significant because of the low activity present and limited measuring time. The activity distribution in different size groups (Israël's classification) of the environmental aerosols in our experiments in Stockholm shows excellent agreement with the results published by Mohnen & Stierstadt in München although the climatic and geographical conditions are quite different. A comparison of our results in the form of the integral activity distribution curves with that of other investigators shows that the results can be divided in two groups. The results by Schumann (1963) and Wieser (1966) using a Goetz-Aerosol-Spectrometer are in mutual agreement as are the results of Mohnen and Stierstadt (1963) and our measurements both made by an electrical mobility analyzer. It is difficult to know whether the reasons are the different methodologies only or the aerosol composition too.

From the activity spectrum $A(r)$ the relative particle size distribution spectrum $N(r)$ is calculated. We have found, that most of our particle size distribution curves are not unambiguously characterized by a significant peak as expected from the Junge's model (1962) and from other investigations. The particle size distribution curves seem to increase in the region $r < 10^{-6}$ cm. That means either that Junge's model is not fully valid for this size range or that the particle concentration in this size region is changing frequently and influencing the various profiles of the relative particle size distribution curves. It is therefore to be recommended that this dilemma should be cleared up but another non-electrical method estimating all particles in total (charged and uncharged) in the region below $r < 10^{-6}$ cm would be necessary.

Acknowledgements

The senior author wishes to express his sincere thanks to Professor B. Lindell, Director of the National Institute of Radiation Protection in Stockholm, Sweden, who offered him the hospitality of this institute. Thanks are also due to many other persons from this institute who assisted with various phases of this work. The authors are grateful to Dr G. Schumann, Chief of the Department of Environmental Radioactivity of the Second Institute of Physics, University of Heidelberg, West Germany, for valuable discussions in theoretical problems and in the evaluation of the experiments.

REFERENCES

Baust, E. 1967. Die Anlagerung von radioaktiven Atomen und Ionen an Aerosolteilchen. *Z. Phys. 199*, 187–206.

Baust, E. 1967. Die Verwendbarkeit des Goetzschen Aerosolspektrometers zur Messung von Grössenspektren polydisperser Aerosole. *Staub 27*, 180–185.

Bricard, J. 1965. Action of radioactivity and of pollution upon parameters of atmospheric electricity. *Problems of atmospheric and space electricity* (ed. S. C. Coroniti). Elsevier, Amsterdam.

Chamberlain, A. C. & Dyson, E. D. 1956. The dose to the trachea and bronchi from the decay products of radon and thoron. *Brit. J. Radiol. 29*, 317–325.

Evans, R. D. 1955. *The atomic nucleus*, p. 516. McGraw-Hill, New York.

Fuchs, N. A. 1963. On the stationary charge distribution on aerosol particles in a bipolar ionic atmosphere. *Geofis. Pur. Appl. 56*, 185–193.

Gillespie, T. & Langstroth, G. O. 1952. Coagulation and deposition in still aerosols of various solids. *Canad. J. Chem. 30*, 1003–1011.

Goetz, A. & Kallai, T. 1962. Instrumentation for determining size- and mass-distribution of submicron aerosols. *J. Air Poll. Contr. Ass. 12*, 479–486.

Goetz, A. & Preining, O. 1961. Bestimmung der Grössenverteilung eines Aerosols mittels des Goetzschen Aerosolspektrometers. *Acta Phys. Austr. 14*, 292–304.

Gunn, R. 1955. The statistical electrification of aerosols by ionic diffusion. *J. Coll. Sci. 10*, 107–118.

Hasenclever, D. & Siegmann, H. Ch. 1960. Eine neue Methode der Staubmessung mittels Kleinionenanlagerung. *Staub 20*, 212–218.

Holl, W. & Mühleisen, R. 1955. On the equilibrium of ionisation in air containing nuclei. *Geofis. Pur. Appl. 31*, 115–118.

Hursh, J. B. & Lovaas, A. I. 1967. Preparation of a dry ^{228}Th source of thoron. *J. Inorg. Nucl. Chem. 29*, 399–400.

Israël, H. 1957. *Atmosphärische Elektrizität*, Teil I., pp. 156, 287–288. Geest & Portig, Leipzig.

Jacobi, W. 1961. Die Anlagerung von natürlichen Radionukliden an Aerosolpartikel und Niederschlagselemente in der Atmosphäre. *Geofis. Pur. Appl. 50*, 260–277.

Junge, Ch. 1953. Die Rolle der Aerosole und der gasförmigen Beimengungen der Luft im Spurenstoffhaushalt der Troposphäre. *Tellus 5*, 1–26.

Junge, Ch., 1955. The size distribution and aging of natural aerosols as determined from electrical and optical data on the atmosphere. *J. Meteor. 12*, 13–25.

Junge, Ch., 1962. Radioactive Aerosole. *Nuclear Radiation in Geophysics* (ed. H. Israël & A. Krebs), pp. 169–201. Springer-Verlag, Berlin.

Kawano, M. & Nakatani, S. 1961. Size distribution of naturally occurring radioactive dust measured by a cascade impactor and autoradiography. *Geofis. Pur Appl. 50*, 243–248.

Keith, C. H. & Derrick, J. C. 1960. Measurement of the particle size distribution and concentration of cigarette smoke by the "Conifuge". *J. Coll. Sci. 15*, 340–356.

Keefe, D., Nolan, P. I. & Rich, T. A. 1959. Charge equilibrium in aerosols according to the Boltzmann law. *Proc. Roy. Irish Acad. 60A*, 27–45.

Lassen, L. & Rau, G. 1960. Die Anlagerung radioaktiver Atome an Aerosole (Schwebestoffe). *Z. Phys. 160*, 504–519.

Lassen, L. 1961. Die Anlagerung von Zerfallsprodukten der natürlichen Emanationen an elektrisch geladene Aerosole. *Z. Phys. 163*, 363–376.

Misaki, U. 1960. Determination of air flow in an ion chamber. *Pap. Met. Geophys., Tokyo 11*, 348–355.

Mohnen, V. & Stierstadt, K. 1963. Die Verteilung der natürlichen Radioaktivität auf das Grössenspektrum des natürlichen Aerosols. *Z. Phys. 173*, 276–293.

Petrausch, D. 1967. *Elektrostatische Abscheidung radioaktiver Aerosole.* Diplomarbeit. Universität Heidelberg.

Reiter, R. & Carnuth, W. 1967. Das Partikelspektrum eines mit Radonfolgeprodukten beladenen Aerosols. *Naturwissenschaften 54*, 40–41.

Salbreiter, H. & Stierstadt, K. 1966. Der Einfluss unipolarer elektrischer Ladungen auf die Beweglichkeit von natürlichem Aerosol *Z. Phys. 196*, 495–503.

Sawyer, F. & Walton, W. H. 1950, The "Conifuge" —a size-separating sampling device for airborne particles. *J. Sci. Instrum. 27*, 272–276.

Schumann, G. 1963. Grössenspektra radioaktiver Aerosole. *Staub 23*, 412–416.

Schumann, G. 1963. Investigation of radon daughters. *J. Geophys. Res. 68*, 3867–3869.

Shapiro, J. 1956. Studies on the radioactive aerosol produced by radon in air. Univ. of Rochester, *Report UR-461.*

Shleien, B., Friend, A. G. & Thomas, H. A. Jr. 1967. A method for the estimation of the respiratory deposition of airborne material. *Health Phys. 13*, 513–517.

Siksna, R. 1963. On the charging of condensation nuclei by air ions. *J. Rech. Atmosph. 1*, 135–144.

Stierstadt, K. & Papp, M. 1960. Aerosole als Träger der natürlichen Radioaktivität. *Atomkernenergie 5*, 459–461.

Stöber, W. 1967. Design and performance of a size-separating aerosol centrifuge facilitating particle size spectrometry in the submicron range. *Assessment of Airborne Radioactivity*, Proceedings of a Symposium, Vienna, 3–7 July 1967, pp. 393–404.

Twomey, S. & Severynse, G. T. 1963. Measurements of size distributions of natural aerosols. *J. Atm. Sci. 20*, 392–396.

Twomey, S. & Severynse, G. T. 1963. Size distributions of natural aerosols below 0.1 micron. *J. Atm. Sci. 21*, 558–564.

Whitby, K. T. 1961. Generator for producing high concentrations of small ions. *Rev. Sci. Instrum. 32*, 1351–1355.

Whitby, K. T. & Clark, W. E. 1966. Electic aerosol particle counting and size distribution measuring system for the 0.015 to 1μ size range. *Tellus 18*, 573–586.

Wieser, P. 1966. Über die Grössenverteilung des natürlichen radioaktiven Aerosols. *Atompraxis 12*, 294–296.

Wilkening, M. H. 1952. Natural radioactivity as a tracer in the sorting of aerosols according to mobility. *Rev. Sci. Instrum. 23*, 13–16.

РАСПРЕДЕЛЕНИЕ ЕСТЕСТВЕННОЙ РАДИОАКТИВНОСТИ В СУБМИКРОННЫХ ЧАСТИЦАХ АЭРОЗОЛЯ

Для изучения спектра размеров частиц окружающего аэрозоля и распределения их естественной активности в интервале размеров 10^{-5} *см* $> r > 10^{-6}$ *см* был построен анализатор подвижности ионов. Этот анализатор был тщательно проверен на ламинарность потока воздуха внутри аппарата. Количество заряженных частиц аэрозоля, классифицированных в дискретные группы по их подвижности (или размерам), оценивалось по α-радиоактивности собранных частиц, помеченных перед их входом в анализатор ионами *ThB*. Анализатор электрической подвижности ионов завершался струйным диффузионным зарядником для сообщения частицам аэрозоля заряда одного знака. Электрические параметры этого прибора проверялись, чтобы убедиться в надёжности его работы. Активационные спектры по размерам $A(r)$ трансформировались в кривые относительных распределений частиц по размерам $N(r)$. Измерения проводились в Стокгольме, Швеция, при изменении физических условий (активации, времени нахождения частиц в приборе, напряжения на коллекторе или применением диффузионного зарядника для однородного по знаку заряжения частиц). Все эксперименты дали весьма сходные результаты. Активационные кривые $A(r)$ положительных и отрицательных частиц имеют аналогичные профили с максимумом в области $r = 3\text{–}6 \cdot 10^{-6}$ *см* в соответствии с моделью Юнге распределения частиц по размерам. Рассчитанные кривые относительных распределений частиц по размерам $N(r)$ не всегда характеризуются максимумом, как можно ожидать из модели Юнге, но часто показывают уменьшение для радиусов $r < 10^{-6}$ *см*, так что пик здесь не проявляется.